Dynamical instability of the motion of atoms in a silicon crystal

Takaya Miyano
Department of Intelligent Machines and System Engineering, Faculty of Science and Technology, Hirosaki University, 3 Bunkyocho, Hirosaki, Aomori 036–8561, Japan

Shinji Munetoh, Koji Moriguchi, and Akira Shintani
Electronics Engineering Laboratories, Sumitomo Metal Industries, Limited, 1-8 Fusocho, Amagasaki, Hyogo 660-0891, Japan
(Received 1 June 1999; revised manuscript received 1 December 2000; published 12 June 2001)

The dynamical nature of the motion of atoms in a silicon crystal is investigated from the information theoretic standpoint with time series analysis about numerical solutions of molecular dynamics simulation. The atomic motion exhibits exponential decay of information entropy with a characteristic time scale of $\sim 40 \times 10^{-15}$ sec. This observation may be interpreted as a signature of microscopic dynamical instability in solids.

DOI: 10.1103/PhysRevE.64.016202 PACS number(s): 05.70.Ln, 05.40.−a, 61.50.−f

I. INTRODUCTION

Deterministic chaos as irregular and unpredictable dynamical behavior despite determinism governing the time evolution of a dynamical system has been discovered in many macroscopic systems. For microscopic systems, in contrast, the existence of deterministic chaos has been an issue of interest to be fixed. Recently Gaspard *et al.* have shown experimental evidence of microscopic chaos for a fluid system [1]. They kept track of erratic motion of a fine particle suspended on deionized water to estimate the probability for the Brownian trajectory to remain within given distances of reference trajectories. Information entropy inferred from the observations was found to decay exponentially with time, which was interpreted as a sign of chaotic behavior of fluid molecules. Such dynamical instability might be expected to exist for the motion of atoms in solids as well. Their approach, however, is not applicable to solids, since the characteristic time scale of atomic motion is of a prohibitive order below the time resolution of the existing experimental apparatus.

In this paper, time series analysis is applied to the motion of atoms in a crystal cell as numerical solutions of molecular dynamics (MD) simulation to investigate dynamical nature of the motion from the information theoretic point of view. MD simulation allows us to look at quick motion of microscopic particles without actual experimental observation and is indispensable for the present work. One might wonder why time series analysis, wherein the underlying dynamics is supposed to be unknown, is utilized to analyze dynamical properties of a fully deterministic system whose governing equations are given beforehand. The present target system, however, is of too many degrees of freedom to carry out direct theoretical analysis of the governing equations. Our goal is to explore microscopic dynamical instability in condensed ordered systems, not the physics of a particular material. In a preliminary work, which has not appeared in a publication, we investigated dynamical behavior of atoms in graphite crystal as a canonical ensemble generated by MD simulation based on a set of Langevin's equations including Tersoff's potential. It was argued, however, that Tersoff's potential may be inappropriate to handle anisotropic systems such as graphite (because of difficulty in reproducing interlayer interactions), in addition that the employed type of thermostat could give rise to false dynamical instability of the atomic motion. To fix these problems, silicon crystal as a microcanonical ensemble free from implementing thermostat is chosen as the target system in this work. Silicon systems are tractable and convenient, in that they allow utilizing Tersoff's potential that has been shown to successfully reproduce elastic properties [2–6] as well as thermodynamic properties [7,8]. The present MD simulation is based on a set of Newton's equations including a particular class of Tersoff's potential.

In time series analysis, we generally need to estimate the dimension and the largest Lyapunov exponent to test for evidence of dynamical instability suggesting possible existence of deterministic chaos. The dimension is related to irreducible degrees of freedom of a dynamical system. The exponent corresponds to the rate at which information will be lost with time from a dynamical system by itself. A standard method to infer the dimension is the Grassberger-Procaccia algorithm [9]. This method, however, has been shown to be able to be fooled by temporally correlated random sequences as a linear stochastic process to induce misdiagnosis about dynamical properties [10]. As shown in this paper, the Grassberger-Procaccia algorithm, as a direct method of estimating the dimension seems to yield no good estimates possibly because of the constraint stemming from the size of data [11]. We instead make use of an indirect approach, i.e., the diagnostic algorithm recently developed by Wayland *et al.* [12] as a simpler variant of the Kaplan-Glass algorithm [13]. This method is based on the fact that visible determinism in dynamical behavior should give rise to smoothness of trajectories reconstructed from a time series in phase space. It allows inferring the dimension indirectly in terms of the diversity of directions of neighboring trajectories. A particular class of randomness that would appear as a linear stochastic process would be detected sensitively by this method.

A standard method to infer the Lyapunov spectrum is the Sano-Sawada algorithm [14]. This method is also presumed to be intractable in this work, when considering degrees of freedom of the target system. As an alternative approach, the mutual information is estimated as a function of time elaps-

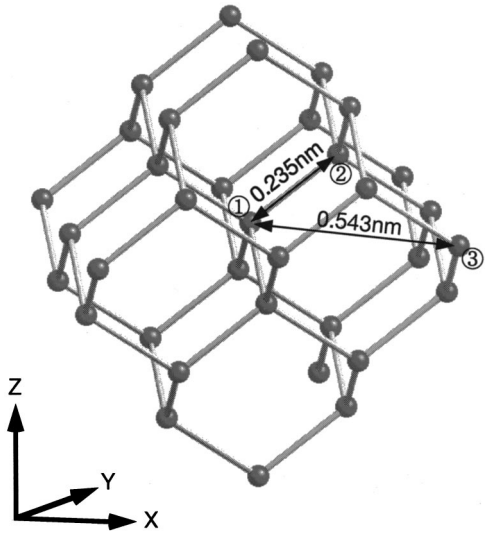

FIG. 1. Schematic diagram of a silicon crystal cell.

ing [15,16]. If there is decay of information entropy with time, a dynamical system can be said to be dynamically unstable. Another popular approach to estimating the largest Lyapunov exponent is the Sugihara-May [17] algorithm based on short-term predictability of deterministic chaos. This algorithm is also utilized in this work. It can detect spontaneous loss of information from a dynamical system in terms of the decay of predictability with time, in time series prediction. The largest Lyapunov exponent can be inferred from the scaling property of the predictive error to the prediction-time interval [18,19]. Unlike the Sano-Sawada and the Sugihara-May algorithms, however, the mutual information can provide information about flows of information entropy in various directions of crystal. Such information is subsidiary to the present objective. Nevertheless, it might be interesting in the sense that it permits examining the dependence of the rate of crystal growth on the crystal direction from the information theoretic point of view.

II. MOLECULAR DYNAMICS SIMULATION

In MD simulations atoms of a dynamical system are viewed as microscopic particles subjected to classical mechanical equations of motion whose potential terms mimic quantum mechanical aspects of the system. The target system of this work is a silicon crystal cell of a size of $1.629 \times 1.629 \times 1.629$ nm^3, consisting of 216 atoms, treated as a microcanonical ensemble. Figure 1 illustrates a schematic diagram of the cell, where atom 1 represents a central atom at a general site and atoms 2 and 3 are its nearest neighbors in the [111] and [100] directions, respectively. Let $\boldsymbol{r}_i(t) = (x_i(t), y_i(t), z_i(t))^T$, ($T$, transpose) be the position vector of the ith atom at time t, determined by the following equation:

$$m_i \frac{d\dot{\boldsymbol{r}}_i(t)}{dt} = -\operatorname{grad} V(\boldsymbol{r}_i(t)), \tag{2.1}$$

where $\dot{\boldsymbol{r}}_i$ expresses the derivative of first order with respect to time and m_i is the mass. V is a Tersoff's potential to simulate interatomic interactions, expressed by the following set of equations [2,3]:

$$E = \frac{1}{2} \sum_{i \neq j} V(r_{ij}), \tag{2.2}$$

$$V(r_{ij}) = f_c(r_{ij})[f_R(r_{ij}) + b_{ij} f_A(r_{ij})], \tag{2.3}$$

$$f_R(r_{ij}) = A_{ij} \exp(-\lambda_{ij} r_{ij}), \tag{2.4}$$

$$f_A(r_{ij}) = B_{ij} \exp(-\mu_{ij} r_{ij}), \tag{2.5}$$

$$f_c(r_{ij}) = \begin{cases} 1 & (r_{ij} < R_{ij}), \\ \frac{1}{2} + \frac{1}{2}\cos\left[\frac{\pi(r_{ij} - R_{ij})}{S_{ij} - R_{ij}}\right] & (R_{ij} \leqslant r_{ij} \leqslant S_{ij}), \\ 0 & (r_{ij} > S_{ij}), \end{cases} \tag{2.6}$$

$$b_{ij} = \chi_{ij}(1 + \beta_i^n \zeta_{ij}^n)^{-1/2n}, \tag{2.7}$$

$$\zeta_{ij} = \sum_{\kappa \neq i,j} f_c(r_{ik}) g(\theta_{ijk}), \tag{2.8}$$

$$g(\theta_{ijk}) = 1 + \frac{c_i^2}{d_i^2} + \frac{c_i^2}{d_i^2 + (h_i - \cos\theta_{ijk})^2}, \tag{2.9}$$

$$\lambda_{ij} = \frac{\lambda_i + \lambda_j}{2}, \tag{2.10}$$

$$\mu_{ij} = \frac{\mu_i + \mu_j}{2}, \tag{2.11}$$

$$A_{ij} = \sqrt{A_i + A_j}, \tag{2.12}$$

$$B_{ij} = \sqrt{B_i + B_j}, \tag{2.13}$$

$$R_{ij} = \sqrt{R_i R_j}, \tag{2.14}$$

$$S_{ij} = \sqrt{S_i S_j}. \tag{2.15}$$

Here E is the total energy of the system, given by the sum of $V(r_{ij})$ as a nonlinear function of the distance r_{ij} between the ith and the jth atoms. $V(r_{ij})$ is composed of the repulsive term f_R and the attractive term f_A each multiplied by continuous and smooth cutoff function f_c that determines the working range of the potential to drastically reduce computational burden. Interactions between atoms at a distance exceeding the cutoff distance S_{ij} are neglected. The bond-order coefficient b_{ij} implements many-body effect on the attractive term in the sense that it simulates the influence of the i-k valence bond (the valence bond between the ith and kth atoms) on the i-j valence bond in accordance with the angle θ_{ijk} between the bonds. Thus three-body interactions including an outlying atom beyond S_{ij} can be incorporated into the potential through the angular interactions between adjacent

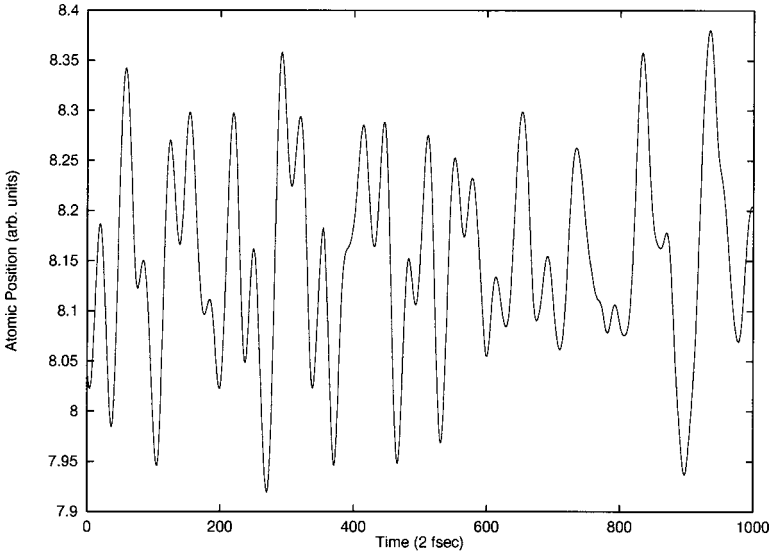

FIG. 2. First 1000 data points of $\{x_1(t)\}$.

bonds. Tersoff's potential can simulate interatomic interactions in isotropic systems. However, it may not be able to mimic interatomic interactions in anisotropic systems such as graphite crystal where carbon atoms take the sp^2 hybrid orbital configuration, which rendered our previous work on graphite crystal to be less reliable.

Each parameter specifying the potential was determined so as to reproduce the cohesive energy of polymorphic silicon crystals as well as static properties of the diamond structure such as the elastic constant and the bond length [2], given as

$$A_i = 1.8308 \times 10^3 \ \text{eV} \quad (i = 1, \ldots, N_{atoms}),$$

$$B_i = 4.7118 \times 10^2 \ \text{eV},$$

$$\lambda_i = 2.4799 \times 10^{10} \ \text{m}^{-1},$$

$$\mu_i = 1.7322 \times 10^{10} \ \text{m}^{-1},$$

$$\beta_i = 1.1000 \times 10^{-6},$$

$$n = 7.8734 \times 10^{-1},$$

$$c_i = 1.0039 \times 10^5,$$

$$d_i = 1.6217 \times 10^1,$$

$$h_i = -5.9825 \times 10^{-1},$$

$$R_i = 2.7 \times 10^{-10} \ \text{m},$$

$$S_i = 3.0 \times 10^{-10} \ \text{m}.$$

These parameters have been shown to successfully reproduce the dispersion curves of lattice vibration for the diamond phase of silicon [5].

Numerical solutions are obtained using Verlet's algorithm [20] under a periodic boundary condition. At the initial stage of calculation, the atoms are arranged at each site of perfect crystal, and crystal temperature is kept constant at 1000 K by means of velocity scaling [21] at every time step of MD simulation (during 50 000 MD steps) until stationarity of the bond energy is achieved. One MD step corresponds to 2×10^{-15} sec (2 fsec). Then alternatively the total energy is kept constant without the velocity scaling. We thus obtain time series data consisting of 10 000 data points over 10 000 MD steps. Figure 2 shows, for instance, the first 1000 data points of $\{x_1(t)\}_{t=1}^{10\,000}$ $(t \in \mathbb{N})$ for atom 1. Frequency power spectra estimated from the time series have a broad-band structure, suggesting that the atomic motion contains irregular ingredients. Estimated phonon dispersion relation curves indicate optical phonon about 15 THz.

III. DYNAMICAL ANALYSIS AND DISCUSSION

We may view the motion of an atom as a signal emanating from an information source, and its adjacent atoms as receivers of the signal through the interactions between atoms. Then the association between positions of a central and its adjacent atom may reflect information transfer through the chemical bond as a communication channel. Information transfer between neighboring atoms as well as spontaneous loss of information from the signal can be measured in terms of the mutual information [15,16]. Let $U = \{u(t)\}_{t=1}^{N}$ and $V = \{v(t)\}_{t=1}^{N}$ be time series of N data points as sets of realizations of random variables u and v, respectively. The average mutual information $I(V;U)$ expressing the amount of information that one can acquire about V, given that U has been known, is defined as

$$I(V;U) = H(V) - H(V|U) = H(U) + H(V) - H(U,V), \tag{3.1}$$

where $H(U)$ and $H(U,V)$ denote the information entropy and the joint information entropy, respectively, expressed as

$$H(U) = -\sum_{u \in U} P(u) \log_2 P(u), \tag{3.2}$$

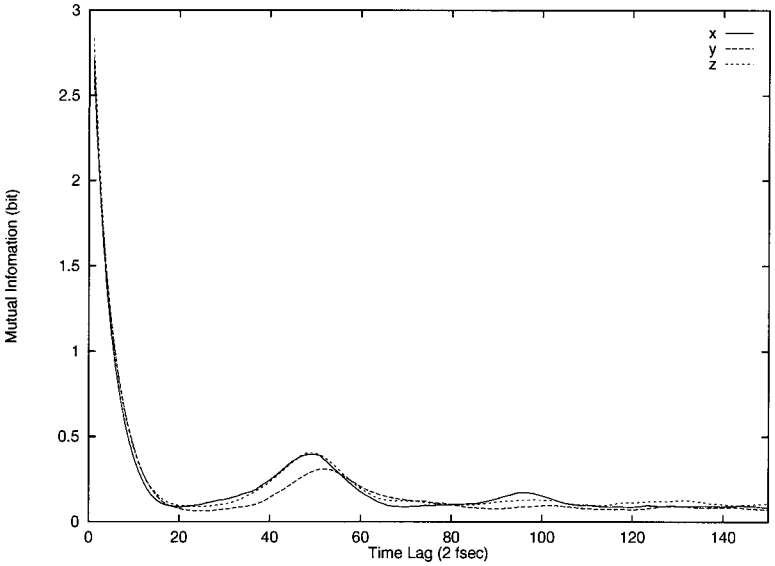

FIG. 3. Average mutual information between $x_1(t),y_1(t),z_1(t)$ and $x_1(t+\Delta t),y_1(t+\Delta t),z_1(t+\Delta t)$, respectively.

$$H(U,V)=-\sum_{u\in U,v\in V}P(u,v)\log_2 P(u,v). \qquad (3.3)$$

$P(\cdot)$ and $P(\cdot,\cdot)$ are the probability function and the joint probability function, respectively. When V is replaced by time-delayed realizations of $u(t)$, i.e., $v(t)=u(t+\Delta t)$, $I(V;U)$ provides a measure for spontaneous loss of information with time-elapsing Δt. In the present work the probability functions are approximated by one-dimensional and two-dimensional histograms each consisting of 256 equisized partitions and of 256×256 equisized partitions.

Figure 3 shows the average mutual information as a function of Δt between $x_1(t),y_1(t),z_1(t)$ and $x_1(t+\Delta t),y_1(t+\Delta t),z_1(t+\Delta t)$, respectively. The mutual information decreases exponentially to reach a minimum at a time lag of 40×10^{-15} sec (40 fsec, 20 MD steps). No significant dependence on the direction of motion can be seen, as expected from the isotropic structure of the crystal. Weak peaks about 100 fsec (10 THz, 50 MD steps) and about 200 fsec (5 THz, 100 MD steps) may correspond to lattice vibrations conveying a certain amount of information through the synchronized motion of atoms. Initial rapid decay of the mutual information indicates that infinitesimal difference between initial conditions will grow into a finite magnitude in the course of time. That is, the system loses memory about initial conditions very quickly. There is spontaneous and exponential loss of information from the system with a characteristic time scale of ~40 fsec, which can be interpreted as a signature of dynamical instability.

Figure 4 shows the average mutual information between $x_1(t),y_1(t),z_1(t)$ and $x_2(t+\Delta t),y_2(t+\Delta t),z_2(t+\Delta t)$, respectively. Atom 2 as the nearest neighbor in the [111] direction is directly bonded to atom 1 at a distance of 0.235 nm. The average mutual information between $x_1(t),y_1(t),z_1(t)$ and $x_3(t+\Delta t),y_3(t+\Delta t),z_3(t+\Delta t)$ is shown in Fig. 5. Atom 3 as the nearest neighbor in the [100] direction is not directly bonded to atom 1 at a distance of 0.543 nm. In each crystal direction, information transfer is as small as the value to which the mutual information decays in Fig. 3. It is difficult to give a physical explanation to particu-

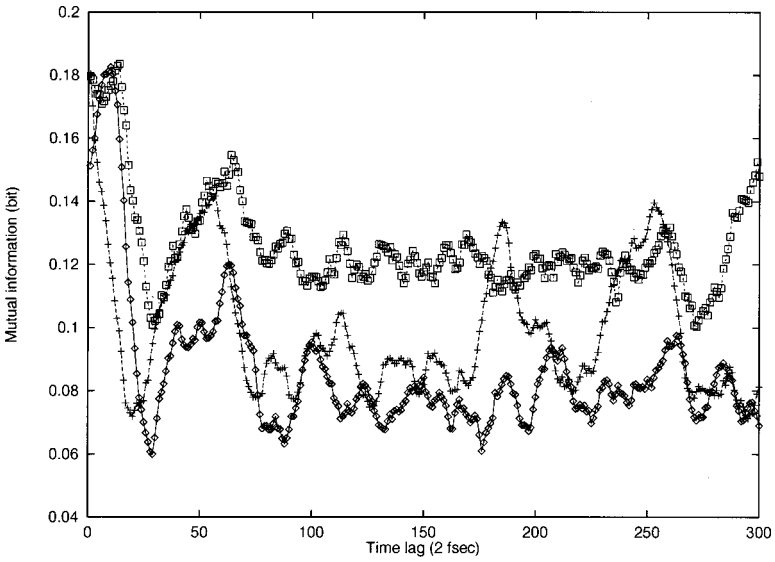

FIG. 4. Average mutual information between $x_1(t),y_1(t),z_1(t)$ and $x_2(t+\Delta t),y_2(t+\Delta t),z_2(t+\Delta t)$, respectively, for neighboring atoms in the [111] direction. Estimates are indicated by $\diamond$, $+$, and $\square$ for x,y, and z component, respectively.

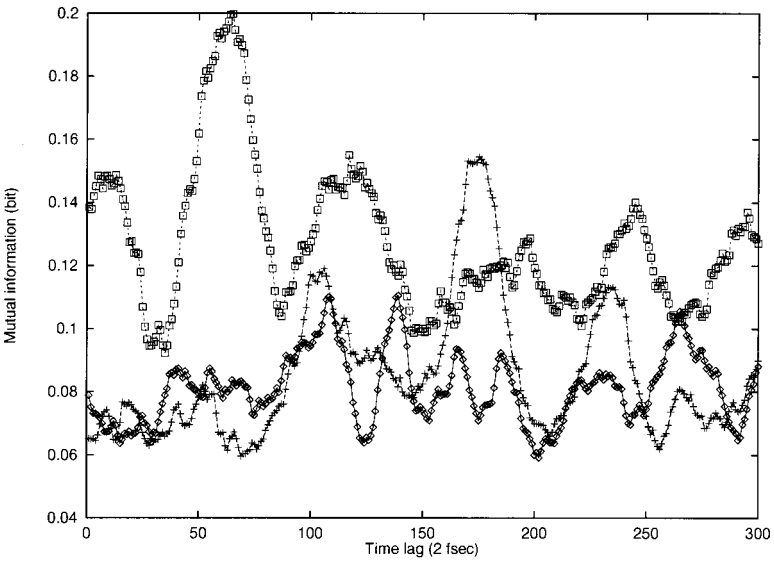

FIG. 5. Average mutual information between $x_1(t), y_1(t), z_1(t)$ and $x_3(t+\Delta t), y_3(t+\Delta t), z_3(t+\Delta t)$, respectively, for neighboring atoms in the [100] direction. Estimates are indicated by $\diamond$, $+$, and $\square$ for x, y, and z component, respectively.

lar structures of variations of information transfer about the mean level. However, an interesting finding for Figs. 4 and 5 is that the broad behavior and the mean level of information transfer over a time lag of 300 MD steps are much the same between neighboring atoms in the [111] and the [100] directions despite the difference in interatomic distance. When thinking of the relative difference, i.e., 0.235/0.543, the information transfer in the [100] direction may approximately double the amount in the [111] direction. The information transfer may play an important role in the formation of ordered structure in the arrangement of atoms. In this sense the flow of information entropy may contribute to the rate of crystal growth. Hence crystalline structure would grow faster in the [100] direction in hypothetical competition of crystal growth. This conjecture seems to agree with the experimental fact that the rate of crystal growth in the [100] direction is larger than that in the [111] direction in solid phase epitaxial growth on silicon crystalline substrates [22].

The signature of dynamical instability that has appeared in the decay of the mutual information is confirmed by virtue of the Sugihara-May algorithm. In this method we first construct phase space with lagged sequences of data points from a time series $\{u(t)\}_{t=1}^{N}$ as

$$\boldsymbol{u}(t)=(u(t),u(t-\Delta t),\ldots,u[t-(D-1)\Delta t])^T, \quad (3.4)$$

where Δt is an appropriate time lag and D denotes the embedding dimension. Predictions T time steps into the future can be made by means of function approximation of dynamical behavior

$$u(t+T\Delta t)=F(\boldsymbol{u}(t))+\epsilon(T\Delta t), \quad (3.5)$$

where F is approximating function and $\epsilon(T\Delta t)$ denotes random variables representing the predictive error. A Sugihara-May predictor, referred to as a nonlinear local approximation technique, is utilized to construct the approximating function [17,19]. In this predictive method library examples as pairs of $\boldsymbol{u}(t)$ and $u(t+T\Delta t)$, representing the dynamical behavior of a time series, are usually generated from the first half of the series. The corresponding future values are forecast for $\boldsymbol{u}(t_p)$ generated from the remaining part of the series by the following procedure. From the library examples, we first find $D+1$ closest vectors $\boldsymbol{u}(t_k)$ $(k=1,\ldots,D+1)$ pointing the vertices of the smallest simplex that includes $\boldsymbol{u}(t_p)$ in the D-dimensional Euclidean space. We then make predictions $\hat{u}(t_p+T\Delta t)$ by calculating a weighted sum of the basis examples $u(t_k+T\Delta t)$:

$$\hat{u}(t_p+T\Delta t)=\frac{\sum_{k=1}^{D+1} u(t_k+T\Delta t)\exp(-d_k)}{\sum_{k=1}^{D+1}\exp(-d_k)}, \quad (3.6)$$

$$d_k=|\boldsymbol{u}(t_p)-\boldsymbol{u}(t_k)|. \quad (3.7)$$

The predictive error is inevitable in a function approximation with sparse examples for any dynamical behavior. A remarkable feature of chaos, however, is that the separation of predicted dynamical behavior from actual one with the prediction-time interval is immense due to the instability intrinsic to the underlying dynamics. Hence exponential increase in the predictive error with T can be an indication of chaotic dynamics. The rate of decay of predictability is ascribed to the largest Lyapunov exponent λ_{max} as the rate of separation of nearby trajectories in the most unstable direction in the phase space. Thus λ_{max} can be inferred from the scaling property of the predictive error $\epsilon(\cdot)$ [18,19]:

$$\epsilon(T\Delta t)=\epsilon(\Delta t)\exp[\lambda_{max}(T-1)\Delta t]. \quad (3.8)$$

That is, λ_{max} can be estimated as the initial slope of semilog plot of $\ln[\epsilon(T\Delta t)/\epsilon(\Delta t)]$ against $(T-1)\Delta t$.

Figure 6 shows Sugihara-May tests for $\{x_1(t)\}$, $\{y_1(t)\}, \{z_1(t)\}$. Library examples are generated from the first 5000 data points. Forecasts are made for the remaining part of the data. The predictive error is measured in terms of the root mean square error between predicted and actual values normalized by the standard deviation of the actual val-

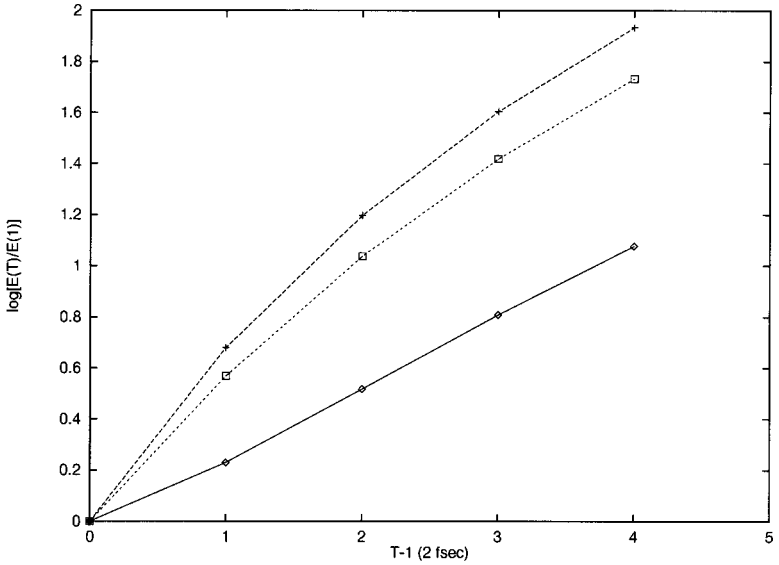

FIG. 6. Semilog plots of $\log[\epsilon(T\Delta t)/\epsilon(\Delta t)]$ against $(T-1)\Delta t$ for the motion of the atom 1 ($D=3, \Delta t=2$ fsec). $\epsilon(\cdot)$ denotes the normalized root mean square error. Estimates are indicated by $\diamond$, $+$ and $\square$ for x, y, and z component, respectively.

ues. To observe initial decay of predictability as precisely as possible, Δt is set to 1 MD step (2 fsec). The embedding dimension is chosen as $D=3$ at which $\epsilon(\Delta t)$ as a function of D is minimum [$\epsilon(\Delta t)=0.074, 0.027, 0.037$ for x, y, and z component]. There can be seen rapid decay of predictability for each component. Linear fitting of the semilog plots provides estimates of $\lambda_{max}=0.2731$, 0.4792, 0.4315 (2 fsec)$^{-1}$, where linear correlation of the fitting is 0.9985, 0.9798, 0.9866 for x, y, and z component. Thus the largest Lyapunov exponent can be said to be positive. However, the origin of the discrepancies in the estimates of λ_{max} is unclear.

To infer degrees of visible determinism in the atomic motion, we next make use of the diagnostic algorithm of Wayland *et al.* The heart of this algorithm is that neighboring trajectories generated from a time series in phase space should point in similar directions if determinism is visible in the series. Phase space is constructed in the same way as the Sugihara-May algorithm. For a randomly chosen vector $\boldsymbol{u}(t_0)$, we first find K nearest neighbors $\boldsymbol{u}(t_k)$, then make the image of each vector as $\boldsymbol{u}(t_k+T\Delta t)$ $(k=0,1,\ldots,K)$ with appropriately chosen time interval $T\Delta t$. The diversity of directions of neighboring trajectories can be measured in terms of the translation error

$$E_{trans}=\frac{1}{K+1}\sum_{k=0}^{K}\frac{\|\boldsymbol{v}(t_k)-\langle\boldsymbol{v}\rangle\|^2}{\|\langle\boldsymbol{v}\rangle\|^2}, \tag{3.9}$$

$$\langle\boldsymbol{v}\rangle=\frac{1}{K+1}\sum_{k=0}^{K}\boldsymbol{v}(t_k), \tag{3.10}$$

$$\boldsymbol{v}(t_k)=\boldsymbol{u}(t_k+T\Delta t)-\boldsymbol{u}(t_k). \tag{3.11}$$

The more visible the determinism is, the smaller the E_{trans}. To reduce the stochastic error of estimates, we seek the medians of E_{trans} for Q sets of M randomly chosen $\boldsymbol{u}(t_0)$ and then estimate the mean of the Q medians [12]. According to previous numerical work [19], E_{trans} does not exceed ~ 0.1 for deterministic time series such as finite-dimensional

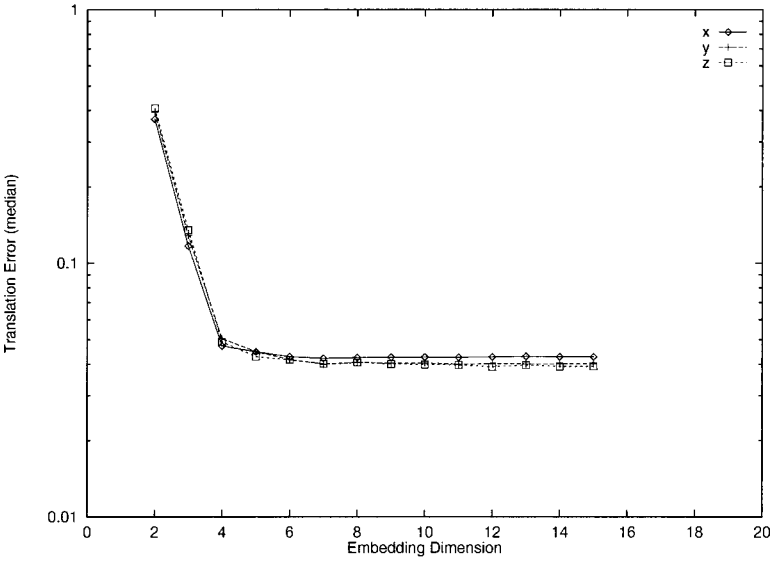

FIG. 7. Wayland tests on the motion of atom 1 ($T=5, K=4, Q=20$). Estimates are indicated by $\diamond$, $+$ and $\square$ for x, y,, and z component, respectively.

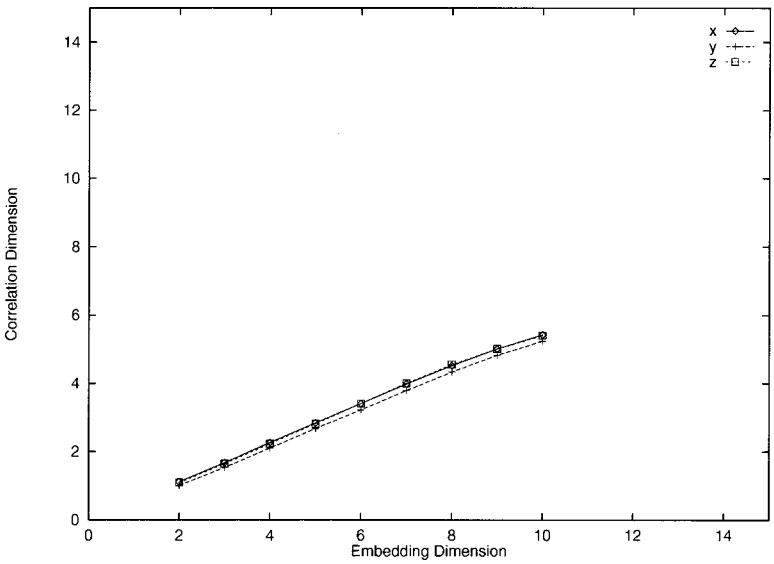

FIG. 8. Correlation dimension as a function of the embedding dimension for the motion of atom 1. Embedding is performed at a time lag of $\Delta t = 10$ MD steps. Estimates are indicated by $\diamond$, $+$, and $\square$ for x,y, and z component, respectively.

chaos, while E_{trans} lies over ~ 0.5 for temporally correlated random noises with various fractional power law spectral indices ($0 \leqslant \alpha \leqslant 2$). It takes ~ 1 independently of the embedding dimension for uncorrelated random noise.

Wayland tests for $\{x_1(t)\},\{y_1(t)\},\{z_1(t)\}$ are shown in Fig. 7. Δt is set to 10 MD steps from Fig. 3 in accordance with the prescription proposed in Ref. [15]. There can be seen no significant dependence on the direction of motion. The translation error reaches a minimum at $D=7$ and subsequently keeps constant. This implies that crossings of trajectories due to inappropriate choice of the embedding dimension is substantially diminished at and above $D=7$, which results in clearly visible determinism like finite-dimensional chaos. Reconstructed trajectories look smooth at and above $D=7$. Hence the dimension is inferred to be greater than seven. The observed dynamical instability is not ascribed to a class of randomness that can be viewed as a linear stochastic process, i.e., possibly very high-dimensional chaos. Finite (not very high) degrees of freedom seem to have an important effect on the dynamical behavior of atoms. However, the dimension, inferred to be greater than seven, may be too large to be estimated by means of the Grassberger-Procaccia algorithm because of paucity of data points ($N=10\,000$). Figure 8 shows estimates of the correlation dimension as a function of the embedding dimension ($\Delta t=10$ MD steps). Linear correlation of the correlation integral as a function of the correlation distance lies between 0.9843 and 0.9999. Although estimated correlation dimension is considerably smaller than the corresponding embedding dimension, no saturation of the correlation dimension with the embedding dimension as the indication of deterministic chaos can be observed. According to Ruelle's prescription [11], we would need at least 10^6 data points to capture such indications. For the present such a large size of data is impractical to carry out numerical analysis.

IV. CONCLUSION

The present numerical analysis has disclosed dynamical instability of the motion of atoms in a silicon crystal, suggesting possible existence of microscopic chaos in condensed, ordered systems with a characteristic time scale of the order 10^{-14} sec. Information theoretic analysis can provide not only evidence of dynamical instability but insight into anisotropy in the rate of crystal growth. The diagnostic algorithm of Wayland *et al.* is effective and tractable to test for degrees of visible determinism from time series data of a small size, despite indirect approach to estimate the dimension. The present approach of dynamical analysis would be useful to examine the influence of defects or impurity atoms introduced to crystal on dynamical properties of the system, which would be an issue of interest in a future work.

[1] P. Gaspard, M.E. Briggs, M.K. Francis, J.V. Sengers, R.W. Gammon, J.R. Dorfman, and R.V. Calabrese, Nature (London) **394**, 865 (1998).
[2] J. Tersoff, Phys. Rev. B **39**, 5566 (1989).
[3] J. Tersoff, Phys. Rev. B **49**, 16 349 (1994).
[4] M. Ishimaru, S. Munetoh, T. Motooka, K. Moriguchi, and A. Shintani, Phys. Rev. B **58**, 12 583 (1998).
[5] K. Moriguchi, and A. Shintani, Jpn. J. Appl. Phys., Part 1 **37**, 414 (1998).
[6] T. Motooka, K. Nishihira, S. Munetoh, K. Moriguchi, and A. Shintani, Phys. Rev. B **61**, 8537 (2000).
[7] L.J. Porter, S. Yip, M. Yamaguchi, H. Kaburaki, and M. Tang, J. Appl. Phys., Part 1 **81**, 96 (1997).
[8] L.J. Porter, J.F. Justo, and S. Yip, J. Appl. Phys., Part 1 **82**, 5378 (1997).
[9] P. Grassberger and I. Procaccia, Phys. Rev. Lett. **50**, 346 (1983).
[10] A.R. Osborne and P. Provenzale, Physica D **35**, 357 (1989).
[11] D. Ruelle, Proc. R. Soc. London, Ser. A **427**, 241 (1990).
[12] R. Wayland, D. Bromley, D. Pickett, and A. Passamante, Phys.

Rev. Lett. **70**, 580 (1993).
[13] D.T. Kaplan and L. Glass, Physica D **64**, 431 (1993).
[14] M. Sano and Y. Sawada, Phys. Rev. Lett. **55**, 1082 (1985).
[15] A.M. Fraser and H.L. Swinney, Phys. Rev. A **33**, 1134 (1986).
[16] A.M. Fraser, IEEE Trans. Inf. Theory **35**, 245 (1989).
[17] G. Sugihara and R.M. May, Nature (London) **344**, 734 (1990).
[18] M. Casdagli, Physica D **35**, 335 (1989).
[19] T. Miyano, Int. J. Bifurcation Chaos Appl. Sci. Eng. **6**, 2031 (1996).
[20] L. Verlet, Phys. Rev. **159**, 98 (1967).
[21] L.V. Woodcock, Chem. Phys. Lett. **10**, 257 (1971).
[22] I.G. Kaverina, V.V. Korobtsov, V.G. Zavodinskii, and A.V. Zotov, Phys. Status Solidi A **82**, 345 (1984).